J Pharmacol Sci **119**, 52 – 63 (2012)

Journal of Pharmacological Sciences

Full Paper

Pharmacological Blockade of I_{Ks} Destabilizes Spiral-Wave Reentry Under β-Adrenergic Stimulation in Favor of Its Early Termination

Sara Kato[1], Haruo Honjo[1,*], Yoshio Takemoto[1], Hiroki Takanari[1,3], Tomoyuki Suzuki[1], Yusuke Okuno[1], Tobias Opthof[2,3], Ichiro Sakuma[4], Shin Inada[5], Kazuo Nakazawa[5], Takashi Ashihara[6], Itsuo Kodama[1], and Kaichiro Kamiya[1]

[1]*Department of Cardiovascular Research, Research Institute of Environmental Medicine, Nagoya University, Nagoya 464-8601, Japan*
[2]*Experimental Cardiology Group, Center for Heart Failure Research, Academic Medical Center, Amsterdam 1105AZ, The Netherlands*
[3]*Department of Medical Physiology, University Medical Center Utrecht, Utrecht 3584CM, The Netherlands*
[4]*Graduate School of Engineering, The University of Tokyo, Tokyo 113-8656, Japan*
[5]*National Cardiovascular Center, Research Institute, Suita 565-8565, Japan*
[6]*Department of Cardiovascular and Respiratory Medicine, Shiga University of Medical Science, Otsu 520-2192, Japan*

Received January 9, 2012; Accepted March 21, 2012

Abstract. We tested a hypothesis that an enhancement of I_{Ks} may play a pivotal role in ventricular proarrhythmia under high sympathetic activity. A 2-dimensional ventricular muscle layer was prepared in rabbit hearts, and action potential signals were analyzed by optical mapping. During constant stimulation, isoproterenol (ISP, 0.1 μM) significantly shortened action potential duration (APD); chromanol 293B (30 μM), a selective I_{Ks}-blocker, reversed the APD shortening. VTs induced in the presence of ISP lasted longer than in the control, and this was reversed by 293B. E-4031 (0.1 μM), a selective I_{Kr}-blocker, did not cause such reversal. Spiral-wave (SW) reentry with ISP was characterized by more stable rotation around a shorter functional block line (FBL) than in the control. After application of 293B, SW reentry was destabilized, and rotation around a longer FBL with prominent drift reappeared. The APD abbreviation by ISP close to the rotation center was more pronounced than in the periphery, leading to an opposite APD gradient (center < periphery) compared with controls. This effect was also reversed by 293B. In conclusion, β-adrenergic stimulation stabilizes SW reentry most likely though an enhancement of I_{Ks}. Blockade of I_{Ks} may be a promising therapeutic modality in prevention of ventricular tachyarrhythmias under high sympathetic activity.
[Supplementary Figures: available only at http://dx.doi.org/10.1254/jphs.12008FP]

Keywords: β-adrenergic stimulation, I_{Ks}, spiral-wave reentry, optical mapping, ventricular tachycardia

Introduction

An enhancement of sympathetic nerve activity is known to facilitate life-threatening ventricular tachycardia/fibrillation (VT/VF) (1, 2). Regardless of the initiating event, spiral-wave (SW) or vortex-type reentry (rotors) has been regarded as the major organizing principle of VT/VF (3, 4). As to the sympathetic modification of SW reentry, however, the information available is still limited, and much remains to be clarified.

The delayed rectifier potassium current (I_K), a major determinant of cardiac action potential duration (APD), is composed of rapidly (I_{Kr}) and slowly (I_{Ks}) activating components. They differ in kinetic properties, rectification characteristics, and sensitivity to drugs (5). Most class III antiarrhythmic drugs currently available, such as dofetilide, sotalol, and nifekalant, prolong APD in a reverse frequency-dependent manner by blockade of I_{Kr} (6,

*Corresponding author. honjo@riem.nagoya-u.ac.jp
Published online in J-STAGE on April 28, 2012 (in advance)
doi: 10.1254/jphs.12008FP

7). This limits their therapeutic potency against tachyarrhythmias. In addition, excessive APD prolongation by pharmacological blockade of I_{Kr} renders a certain proarrhythmic propensity known as drug-induced QT prolongation and torsades de pointes (TdP) (8). I_{Ks} is an attractive alternative antiarrhythmic target for several reasons. I_{Ks} is activated strongly by β-adrenergic stimulation (9, 10), leading to spatially heterogeneous shortening of APD in the mammalian ventricles (11). I_{Ks} accumulates at high stimulation rates because of its slow deactivation kinetics (12, 13). Therefore, APD prolongation by I_{Ks} block does, unlike I_{Kr} block, not show a pronounced reverse frequency-dependence (6, 14, 15). In other words, its class III antiarrhythmic potential is preserved under tachycardia (16).

We hypothesized that an enhancement of I_{Ks} is involved in sympathetic modulation of SW reentry in such a way that it promotes ventricular tachyarrhythmias. In the present study, we investigated the effects of acute application of chromanol 293B (293B), a selective blocker of I_{Ks} (14, 17), on VTs mediated by SW reentry in a 2-dimensional epicardial layer of rabbit ventricular tissue treated with isoproterenol (ISP). E-4031, a selective blocker of I_{Kr} (9), was used as a reference drug.

We show that blockade of I_{Ks} can abolish the proarrhythmic effects of ISP used to mimic high sympathetic tone.

Materials and Methods

Experimental model and optical mapping

The procedures followed were in accordance with institutional guidelines; the study protocol was approved by the Institutional Animal Care and Use Committee at Nagoya University. The experimental model and procedures of optical mapping are essentially the same as reported previously (7, 18 – 21). Isolated rabbit hearts (n = 36) were perfused on a Langendorff apparatus with modified Krebs-Ringer solution at 37°C. Complete atriventricular (AV) block was produced by destruction of the His bundle. A 2-dimensional epicardial layer of ventricular myocardium (approximately 1-mm-thick) was prepared by a cryoprocedure at the endocardium. The tissue was stained with a voltage-sensitive dye, di-4-ANEPPS. Cytochalasin D (10 μM) was applied to minimize motion artifacts. Bipolar electrograms were recorded through widely spaced electrodes to monitor ventricular activation.

The hearts were illuminated by bluish-green light-emitting diodes (LEDs) and fluorescence was recorded with a high-speed digital video camera (Fastcam-Max; Photron, Tokyo) to acquire 10 bit gray scale images (256 × 256 pixels) at a sampling rate of 1,000 frames/s. The acquired image covered the anterolateral surface (30 × 30 mm) of the left ventricle (LV). To reveal the action potential signal, the background fluorescence was subtracted and low-pass filtering was applied (22). Spatial resolution after filtering was 0.1 mm. Isochrone activation maps of 4-ms intervals were generated from the filtered image. When two successive isochrones of 4-ms intervals were superimposed at a single pixel (conduction velocity, CV < 3 cm/s), local conduction block was defined at that site. From normalized action potential signals, time points at 10% depolarization and 90% repolarization were identified, and the interval in between was defined as action potential duration at 90% repolarization (APD_{90}). Wave propagation patterns during VT were analyzed by the phase mapping method (23).

Data were obtained before (control), 20 – 30 min after application of 0.1 μM ISP and 20 – 30 min after additional application of 30 μM 293B or 0.1 μM E-4031. Single effects of 30 μM 293B or 0.1 μM E-4031 were also assessed in some experiments. Our pilot experiments showed that 30 μM 293B and 0.1 μM E-4031 caused a similar APD prolongation in their single effects under constant stimulation at a basic cycle length (BCL) of 200 ms (Table 1).

Measurement of conduction velocity and action potential duration

CV and APD_{90} were measured under constant stimulation from the anterior center of LV free wall at BCLs of

Table 1. Effects of chromanol 293B and E-4031 on basal electrophysiological properties

	APD_{90} (ms)		ERP (ms)	CV (cm/s)	
	BCL 200 ms	BCL 400 ms	BCL 400 ms	BCL 200 ms	BCL 400 ms
Control	142.4 ± 1.7	190.7 ± 4.5	192.2 ± 3.2	51.9 ± 0.4	59.7 ± 1.4
293B (30 μM)	159.1 ± 1.6*	213.6 ± 5.4*	214.6 ± 5.1*	51.9 ± 0.4	60.1 ± 1.4
Control	140.7 ± 4.1	198.3 ± 6.4	186.0 ± 8.1	50.7 ± 0.6	60.6 ± 0.6
E-4031 (0.1 μM)	163.9 ± 2.1*	242.9 ± 5.4*	235.0 ± 11.6*	46.6 ± 2.5	60.5 ± 0.8

Data were obtained before (control) and 20 – 30 min after application of 30 μM chromanol 293B (293B, n = 5) or 0.1 μM E-4031 (n = 6). *P < 0.05 vs. control (Student's paired t-test).

200 and 400 ms. A unipolar electrode made of teflon-coated platinum wire (diameter, 0.1 mm) was used for stimulation. The pulses were 2 ms in duration and had an intensity of 1.2 times diastolic threshold. CV was measured during longitudinal propagation in an 18 × 18 mm square area (the fiber orientation was assumed to be constant over the entire mapped region). CV was calculated from the slope of a linear least-squares fit of the activation time plotted against the distance. The measurement of APD_{90} was made at equally spaced 16 sites covering a 7 × 7 mm square area around the stimulation site (Fig. 1A). The effective refractory period (ERP) was estimated by a standard single extrastimulus protocol.

Induction of VT

Reentrant VTs (≥ 3 nonstimulated excitations) were induced by modified cross-field stimulation. Fourteen basic (S1) stimuli (BCL, 400 ms) were applied to the LV apex through a pair of contiguous bipolar electrodes, and a 20-ms monophasic DC pulse of constant voltage (DS2, 20 V) was delivered through a pair of Ag-AgCl paddle electrodes (7 mm in diameter) placed on the lateral surfaces of both ventricles. The S1-DS2 coupling interval was shortened progressively in 10-ms steps to cover the whole vulnerable window of the S1 excitation. VTs lasting > 5 s were defined as sustained.

Numerical simulation

A rabbit ventricular action potential model originally described by Shannon et al. (24) was used for numerical simulation. For 2-dimensional simulation, a rectangular tissue sheet (4 × 4 cm) consisting of 400 × 400 cell units was constructed with Neuman boundary conditions. The intercellular coupling conductance in the horizontal di-

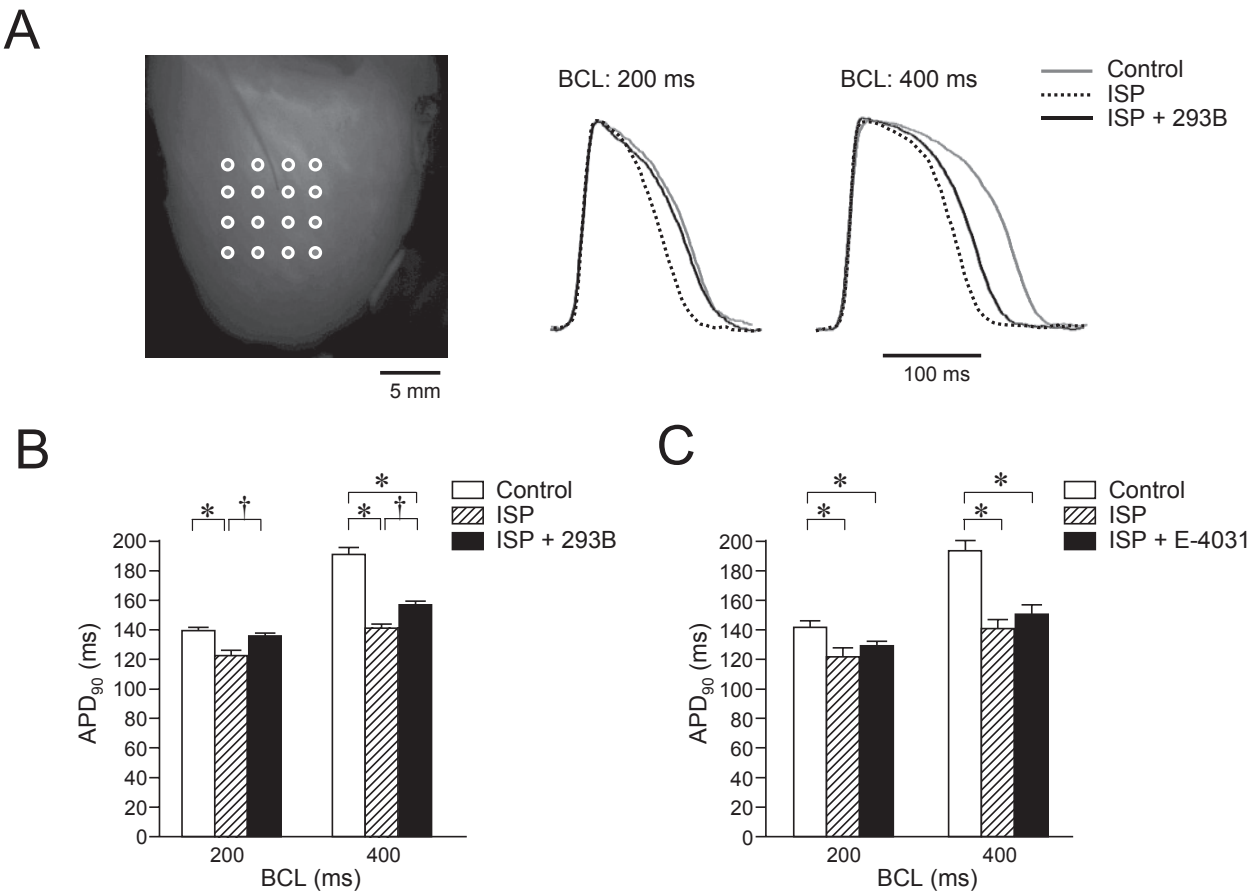

Fig. 1. Effects of isoproterenol (ISP), chromanol 293B (293B), and E-4031 on APD and CV under constant stimulation. CV was measured during longitudinal propagation along the fiber orientation. A: Left, 16 data-sampling sites (circles) for APD measurements covering a 7 × 7 mm area around the stimulation site (LV epicardial surface). Right, averaged action potential signals recorded from the 16 sites before (control), after application of ISP (0.1 μM), and after additional application of 293B (30 μM) at BCLs of 200 and 400 ms. B: Pooled data of APD_{90} obtained from 14 hearts in the control, after ISP (0.1 μM) alone, and after ISP + 293B (30 μM). C: Corresponding pooled data obtained from 6 hearts in the control, after ISP (0.1 μM) alone, and after ISP + E-4031 (0.1 μM). $^{*}P < 0.05$ vs. control, $^{\dagger}P < 0.05$ vs. ISP (ANOVA).

rection was reduced to a tenth (100 nS) of that in the vertical direction (1,000 nS) to create a uniform anisotropy. SW reentry was induced by cross-field stimulation; line stimulation was applied to the left end of the sheet to generate a linear wavefront propagating horizontally and suprathreshold depolarization (1 nA, 5 ms) was given to the top half of the sheet with a variable coupling interval. The effects of ISP at 0.1 μM were represented by an increase in L-type calcium current ($I_{Ca,L}$) by 22%, an increase in I_{Ks} by 286%, and an acceleration of activation/deactivation by 2.5-fold with a hyperpolarizing shift of voltage-dependent activation (by 12.6 mV) of I_{Kr} (10, 25 – 28). 293B at 30 μM was assumed to block I_{Ks} by 50%.

Statistical analyses

Data were expressed as means ± standard error of the mean. Statistical comparisons were performed by ANOVA with the Bonferroni post hoc test or by Student's paired *t*-test when appropriate. Differences were considered significant when $P < 0.05$.

Results

Basal electrophysiological properties

We first examined the effects of 293B (30 μM) and E-4031 (0.1 μM) under constant stimulation in the absence of ISP (Table 1). These drugs caused significant prolongation of APD_{90} without an effect on CV. APD_{90} increased by 17 and 23 ms with 293B at BCLs of 200 and 400 ms, respectively (n = 5, $P < 0.05$), and by 23 and 45 ms with E-4031 at these BCLs (n = 6, $P < 0.05$). ERP increased by 22 ms with 293B (n = 5, $P < 0.05$) and by 49 ms with E-4031 (n = 6, $P < 0.05$) in line with the increases of APD_{90} at a BCL of 400 ms.

We next examined the effects of 293B (30 μM) in the presence of ISP (0.1 μM) (Fig. 1). ISP caused a significant shortening of APD_{90} by 18 and 53 ms at BCLs of 200 and 400 ms, respectively. Additional application of 293B reversed these ISP-induced changes in APD completely at a BCL of 200 ms and partially at 400 ms. We also examined the effects of E-4031 (0.1 μM) in the presence of ISP (0.1 μM). Unlike 293B, E-4031 did not reverse the ISP-induced abbreviation of APD. ISP alone caused a slight but significant increase of CV at BCLs of 200 and 400 ms. The ISP-induced increase of CV remained unaffected by additional application of either 293B or E-4031 (Supplementary Fig. 1: available in the online version only).

Persistence of induced VTs

VTs were induced by modified cross-field stimulation in 25 hearts, and the prevalence of sustained VTs (as a percentage of all VTs) was assessed on the basis of VT episodes/heart (Fig. 2).

Effects of 293B in the presence of ISP were examined in 18 hearts. One or more episodes of sustained VT (lasting > 5 s) occurred in 2/18 hearts in the control, whereas

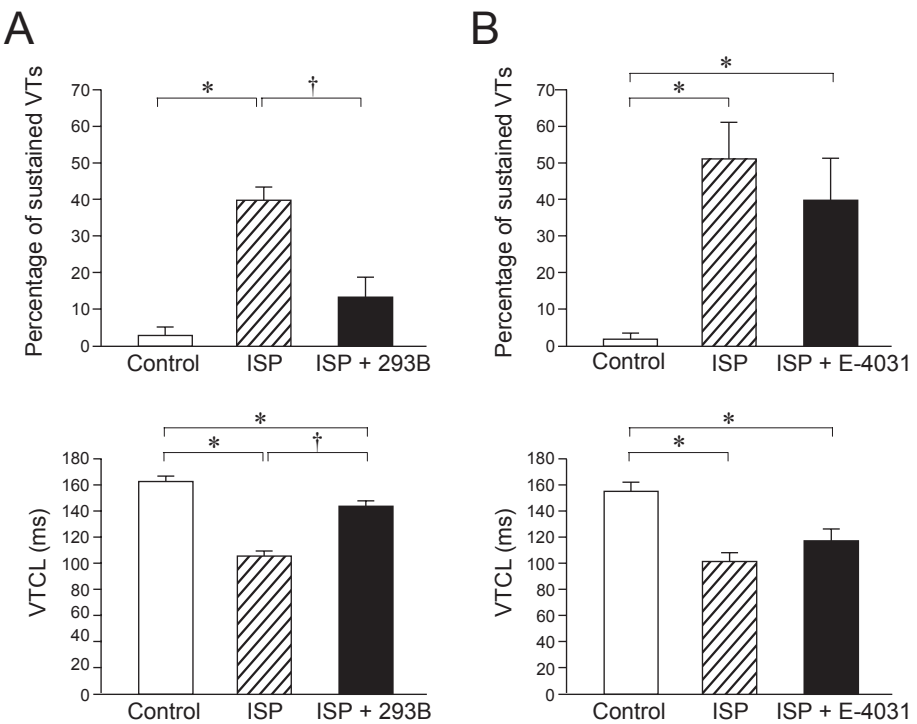

Fig. 2. Effects of isoproterenol (ISP), chromanol 293B (293B), and E-4031 on the incidence of sustained VTs. The incidence of sustained VTs (lasting > 5 s) was assessed on the basis of VT episodes/heart. A: Pooled data obtained from 18 hearts in the control, after ISP (0.1 μM) alone, and after ISP + 293B (30 μM). Top, sustained VTs / all VTs (per heart). Bottom, VT cycle length (VTCL, average of 3 – 10 beats). B: Pooled data obtained from 7 hearts in the control, after ISP (0.1 μM) alone, and after ISP + E-4031 (0.1 μM). Top, sustained VTs / all VTs (per heart); bottom, VTCL (average of 3 – 10 beats). *$P < 0.05$ vs. control, †$P < 0.05$ vs. ISP (ANOVA).

they occurred in 18/18 hearts after application of ISP. The percentage of sustained VTs / all VTs increased significantly from 2.9% ± 2.1% in the control to 38.7% ± 4.3% after application of ISP alone ($P < 0.05$ vs. control). After additional application of 293B, sustained VTs occurred in 8/18 hearts, and the percentage of sustained VTs / all VTs decreased to 14.0% ± 6.0% ($P < 0.05$ vs. ISP).

Effects of E-4031 were examined in 7 hearts. Sustained VTs occurred in 1/7 hearts in the control, whereas they occurred in 7/7 hearts after application of ISP. The percentage of sustained VTs / all VTs increased significantly from 1.1% ± 1.1% in the control to 52.1% ± 9.9% after application of ISP ($P < 0.05$ vs. control). After additional application of E-4031, sustained VTs occurred in 7/7 hearts, and the percentage of sustained VTs / all VTs remained at 40.4% ± 11.6% (ns. compared to ISP). Thus, ISP enhanced the persistence of VT, and the effect was reversed by 293B. E-4031, in contrast, did not reverse the proarrhythmic effect of ISP.

Average VT cycle length (VTCL) decreased significantly from 160 ms at the control to 105 ms after 0.1 μM ISP (Fig. 2). The VTCL prolonged again to 145 ms after additional application of 293B, whereas it remained at 118 ms after additional application of E-4031.

Modification of SW dynamics

Our experiments of VT induction show that ISP-induced enhancement of VT persistence is reversed by 293B. To obtain a mechanistic insight into the antiarrhythmic effect of 293B, we analyzed optical images in 5 hearts exhibiting SW reentry in the observation area during VTs (either sustained or non-sustained) in the control, after application of ISP (0.1 μM) alone, and after additional application of 293B (30 μM).

Figure 3 shows typical data from one heart. Under control conditions, a counterclockwise rotor circulating around a long vertical line of functional block (FBL, 10 – 14 mm in length) can be seen (CL, 146 – 167 ms) during the last three beats before termination (Fig. 3A, left). The rotor drifted upward in a beat-to-beat manner and finally collided with the AV groove. The distant bipolar electrogram (ECG) showed polymorphic excitations terminating shortly (within 2 s). The dynamics of SW reentry was also analyzed by the phase mapping method (23). In the phase map, a phase singularity point (PS) corresponds to the organizing center of SW reentry at a given time. Appearance of PSs reflects formation of SW reentry, whereas disappearance of PSs by collision with either anatomical boundaries or other PSs with opposite chirality indicates termination of SW reentry (23). Under control conditions, a PS moved back and forth along the long FBL before collision with the AV groove (Fig. 3A, right). Figure 3B shows activation patterns during a longer polymorphic VT (lasting 7.3 s) after application of ISP. A more stable counterclockwise rotor (CL, 94-127 ms) was recognized around a short "i" or "j"-shaped FBL (4 – 5 mm) in the LV anterior center. A PS trajectory of three consecutive beats on the phase map exhibited small meandering restricted to the LV anterior center. Figure 3C shows activation patterns during a short polymorphic VT (lasting 2.6 s) after additional application of 30 μM 293B. An unstable counterclockwise rotor (CL, 135 – 141 ms) was recognized around a long FBL with complex configuration (8 – 11 mm). A PS trajectory of the three consecutive beats on the phase map was characterized by a prominent drift before collision with the AV groove.

Qualitatively similar changes of SW reentry were observed after single application of ISP and after additional application of 293B in 4 other hearts. The transformation was characterized by more stabilized rotors around a shorter FBL after single application of ISP and by resumption of unstable rotors around a longer FBL in association with prominent drift after additional application of 293B. Figure 4A illustrates PS trajectories of SW reentry in the four hearts. The length of PS trajectory per unit of time reflects instability of the rotation center. The average length of the PS trajectory per unit of time (1 s) in the 5 hearts decreased significantly from 16.4 ± 2.8 cm in the control to 6.1 ± 1.0 cm after ISP alone ($P < 0.05$) and increased to 10.4 ± 1.3 cm after additional application of 293B ($P < 0.05$ vs. ISP) (Fig. 4B).

Spatial APD_{90} gradient near the rotation center

Previous theoretical studies on SW reentry in 2-dimensional cardiac tissue models have demonstrated spatial gradients of APD, either prolongation (29) or shortening (30) from the periphery to the center. The ISP-induced transformation of SW dynamics (stabilization of rotors) and its reversal by 293B (destabilization of rotors) could be the result of modification of such an APD gradient. We analyzed the spatial gradient of APD_{90} during SW reentry. Action potential signals recorded from 5 points around the rotation center (1.0, 2.0, 4.0, 6.0, and 8.0 mm centrifugal from the PS along the isochronal line of activation) during VTs before (control), after single application of ISP, and after additional application of 293B were compared.

Figure 5A shows representative results. In the control, APD_{90} at 1.0 mm (closest to PS) was longest, and the value decreased gradually as a function of distance from the PS, providing the shortest APD_{90} at 8.0 mm. After application of ISP alone, APD_{90} shortened at all 5 positions. However, the effect was more prominent at sites closer to the PS, leading to an opposite spatial gradient.

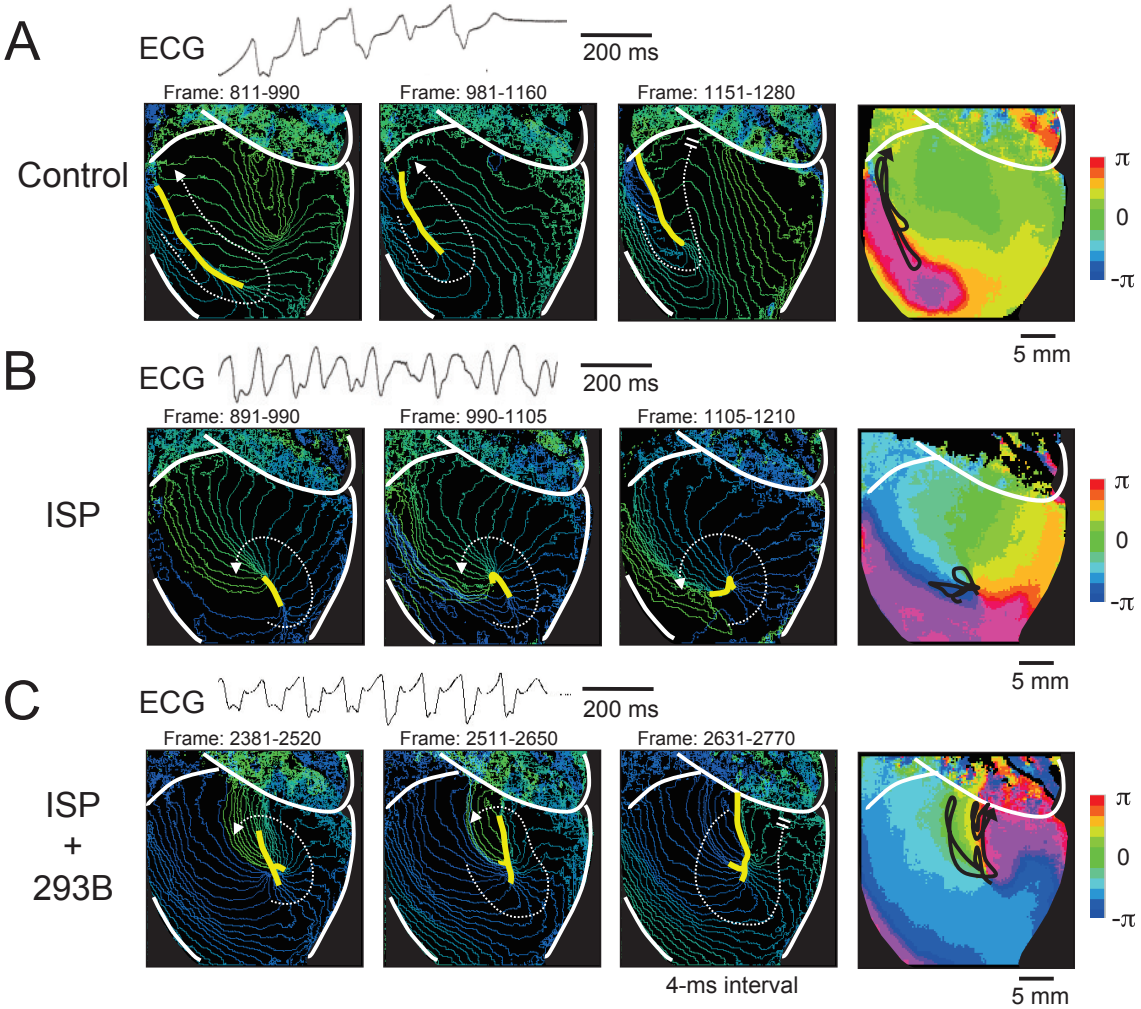

Fig. 3. SW excitations during VT before (control), after application of isoproterenol (ISP, 0.1 μM) alone, and after additional application of chromanol 293B (293B, 30 μM). A: A short polymorphic VT (lasting 1.5 s) under the control condition. Top, bipolar electrogram. Bottom, isochronal activation maps (4-ms intervals with varying colors from blue to green, left) in three consecutive beats and phase map with PS trajectory (black line) during the three beats. An unstable SW circulated counterclockwise around a long FBL (yellow). A PS drifted upward and finally collided with the atrioventricular groove. B: A longer polymorphic VT (lasting 7.3 s) after application of ISP alone. A more stable SW circulated counterclockwise around a short FBL (yellow). A PS trajectory exhibited small meandering restricted to the LV anterior center. C: A short polymorphic VT (lasting 2.6 s) after additional application of 293B. An unstable SW circulated counterclockwise around a long FBL of complex configuration. A PS trajectory showed a prominent drift before collision with the AV groove.

Now, APD_{90} was shortest at 1.0 mm and longest at 8.0 mm. After additional application of 293B, the APD_{90} values prolonged again and the spatial gradient returned toward the situation in the control; APD_{90} was longest at 1.0 mm and shortest at 8.0 mm. Figure 5B summarizes the pooled data obtained from 8 hearts. ISP alone caused significant shortening of APD_{90} at all 5 sites; the closer the distance from PS, the greater the ISP-induced APD shortening. Additional application of 293B caused significant prolongation of APD_{90} at all 5 sites; the closer the distance from PS, the greater the 293B-induced APD prolongation. Thus, ISP creates an opposite APD gradient near the rotation center (center < periphery) compared with the control, and 293B reverses this ISP action.

Numerical model analysis

We analyzed the effects of ISP and 293B on the action potential configuration and the dynamics of SW reentry in mathematical models using action potential equations originally described by Shannon et al. (24) for rabbit ventricular myocytes. The ISP action was mimicked by increases of I_{Ks} and $I_{Ca,L}$ and a modification of activation/deactivation kinetics of I_{Kr}, whereas the 293B action did so by inhibition of I_{Ks}. In the single-cell model under

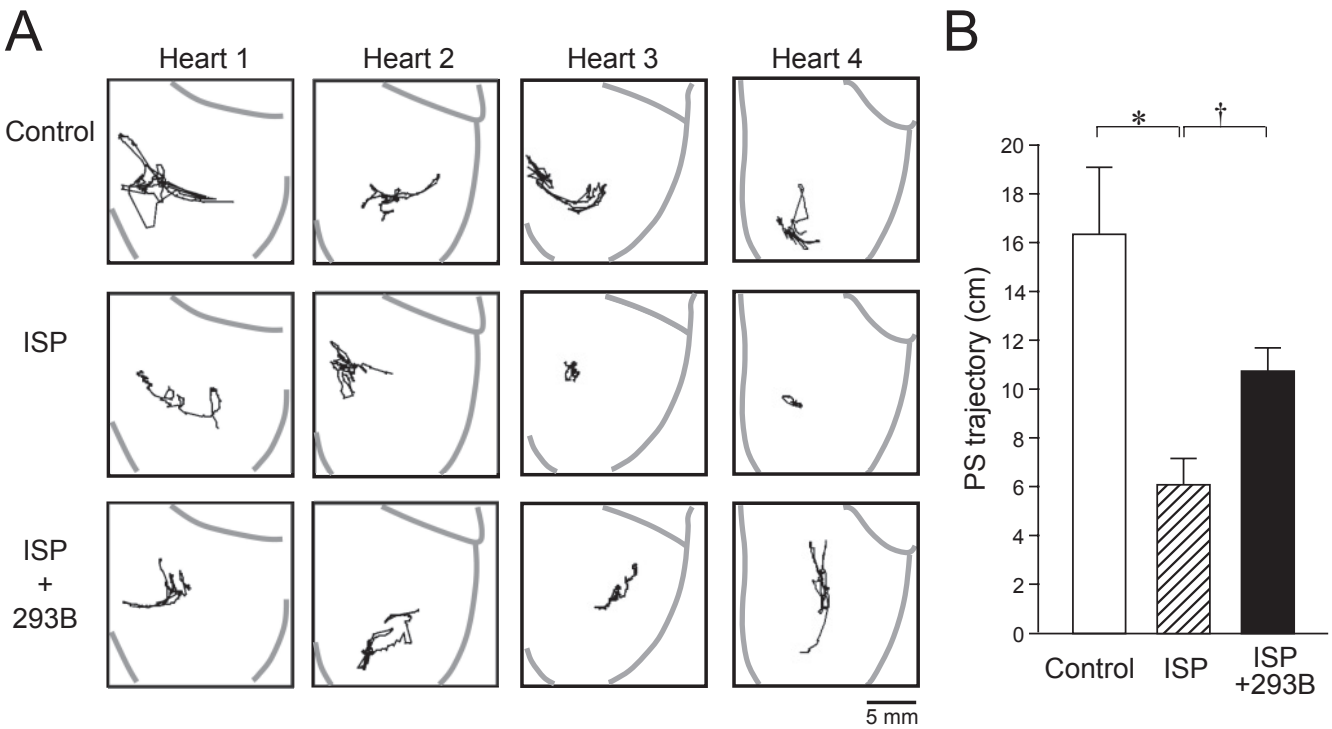

Fig. 4. PS trajectory during VTs before (control), after application of isoproterenol (ISP, 0.1 μM) alone, and after additional application of chromanol 293B (293B, 30 μM). A: PS trajectories in 300 ms during VTs in 4 hearts under control conditions (top), after single application of ISP (middle), and after additional application of 293B (bottom). B: Average length of PS trajectory (n = 5) per unit of time (1 s). *P < 0.05 vs. control, $^{\dagger}P$ < 0.05 vs. ISP (ANOVA).

constant stimulation at BCL 230 ms, ISP shortened APD_{90} by 9% from the control, and additional application of 293B reversed the APD change (Fig. 6A).

In the 2-dimensional model, SW reentry (rotor) was induced by cross-field stimulation and trajectory of PSs was analyzed because its length per unit of time reflects instability of the rotation center (Fig. 6B). In the control, the rotor exhibited meandering and self-terminated by collision with the boundary. ISP stabilized SW reentry in favor of its persistence, and additional application of 293B reversed the ISP action. The APD abbreviation by ISP in the SW reentry circuit was more pronounced near the rotation center, giving rise to an opposite APD gradient (center < periphery) compared with the control, and this effect was also reversed by 293B (Supplementary Fig. 2: available in the online version only). Thus, our major observations in the experiments were reproduced in the mathematical model.

Discussion

Key observations in this study are as follows: 1) Chromanol 293B (30 μM) prolonged APD of rabbit ventricular muscle pretreated with ISP (0.1 μM). 2) VTs induced with ISP lasted longer than those without ISP, and this change was reversed by 293B, but not by E-4031 (0.1 μM). 3) SW reentry was stabilized by ISP leading to its perpetuation, and this ISP action was reversed by 293B. 4) SWs with ISP were associated with an APD gradient (center < periphery), which is opposite to that of the control (center > periphery), and this ISP action was reversed by 293B.

Action potential and conduction properties

Under constant stimulation, ISP (0.1 μM) caused a significant shortening of APD in association with a moderate increase of CV. Additional application of 293B (30 μM) reversed the APD shortening almost completely at a BCL of 200 ms, but partially at 400 ms without affecting CV. These changes can be ascribed to multiple ion channel effects. β-Adrenergic stimulation by ISP is known to increase I_{Ks} and $I_{Ca,L}$ and to modify the activation kinetics of I_{Kr} (10). ISP was also shown to increase outward current carried by chloride (I_{Cl}) (31, 32). In addition to these direct effects on ionic channels, ISP may affect ionic currents indirectly through modification of intracellular Ca^{2+} dynamics. A net increase of outward repolarizing currents is responsible for the ISP-induced

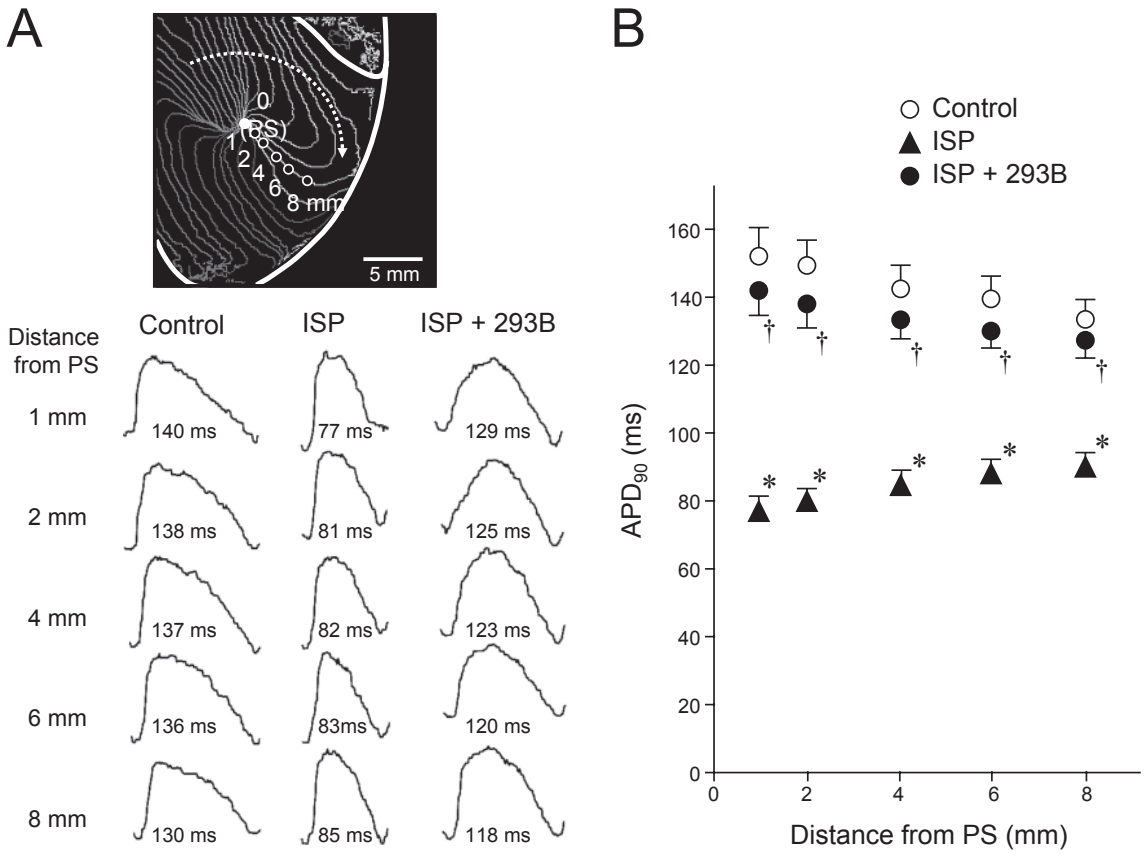

Fig. 5. Spatial APD_{90} gradient near the rotation center. A: Top, five sites of APD_{90} measurement are indicated on the isochrone map of activation during a VT. The distance from the pivot point to the 5 sites is 1.0, 2.0, 4.0, 6.0, and 8.0 mm on the same isochrones. In each experiment, an isochrone was chosen so that 5 action potentials show single full depolarization. Bottom, optical action potential signals at the 5 sites in a heart before (control), after application of isoproterenol (ISP, 0.1 μM) alone, and after additional application of chromanol 293B (293B, 30 μM). APD_{90} value for each action potential is indicated below. B: Pooled data obtained from 8 hearts are plotted against distance from PS. *$P < 0.05$ vs. control, $^{\dagger}P < 0.05$ vs. ISP (ANOVA).

APD abbreviation. I_{Ks} is probably even more important for the APD change at a shorter BCL (200 ms), since it was reversed completely by 293B. Partial reversal of the ISP-induced APD shortening at BCL 400 ms is explained most likely by substantial contribution of I_{Cl} in the APD abbreviation under the slower stimulation rate, where I_{Ks} accumulation is less pronounced.

IC_{50} of 293B to inhibit I_{Ks} in native cardiomyocytes is 1.0 – 1.8 μM (14, 17). 293B was also shown to inhibit the 4-aminopyridine-sensitive transient outward potassium current (I_{to}) at higher concentrations with IC_{50} of 24 – 38 μM (14, 17). There are two types of I_{to} with different inactivation kinetics ($I_{to,fast}$ and $I_{to,slow}$) (5). In rabbit ventricular myocytes, however, only $I_{to,slow}$, which recovers very slowly (time constant of seconds), is present (5). Accordingly, I_{to} is inactivated nearly completely under stimulation at BCLs ≤ 400 ms, and the potential effects of 293B on repolarization via I_{to} inhibition would be negligible.

Our experiments showed that 0.1 μM E-4031, a selective blocker of I_{Kr} (9), did not reverse the APD abbreviation by ISP, although it causes APD prolongation comparable to 30 μM 293B as their single effects (Table 1). Under the condition of β-adrenergic stimulation, where outward currents through I_{Ks} and I_{Cl} are largely augmented, the role of I_{Kr} in the regulation of ventricular repolarization is decreased considerably (9).

The small increase of CV by ISP, which was unaffected by additional application of either 293B or E-4031, could be interpreted as an increase of sodium channel availability and/or by an increase of gap junction conductance in response to ISP, although we did not assess the background of this effect.

VTs of SW reentry

In the present study, VTs were induced by modified cross-field stimulation in the presence of cytochalasin D as an excitation–contraction uncoupler, since modification of steady-state and dynamic action potential configu-

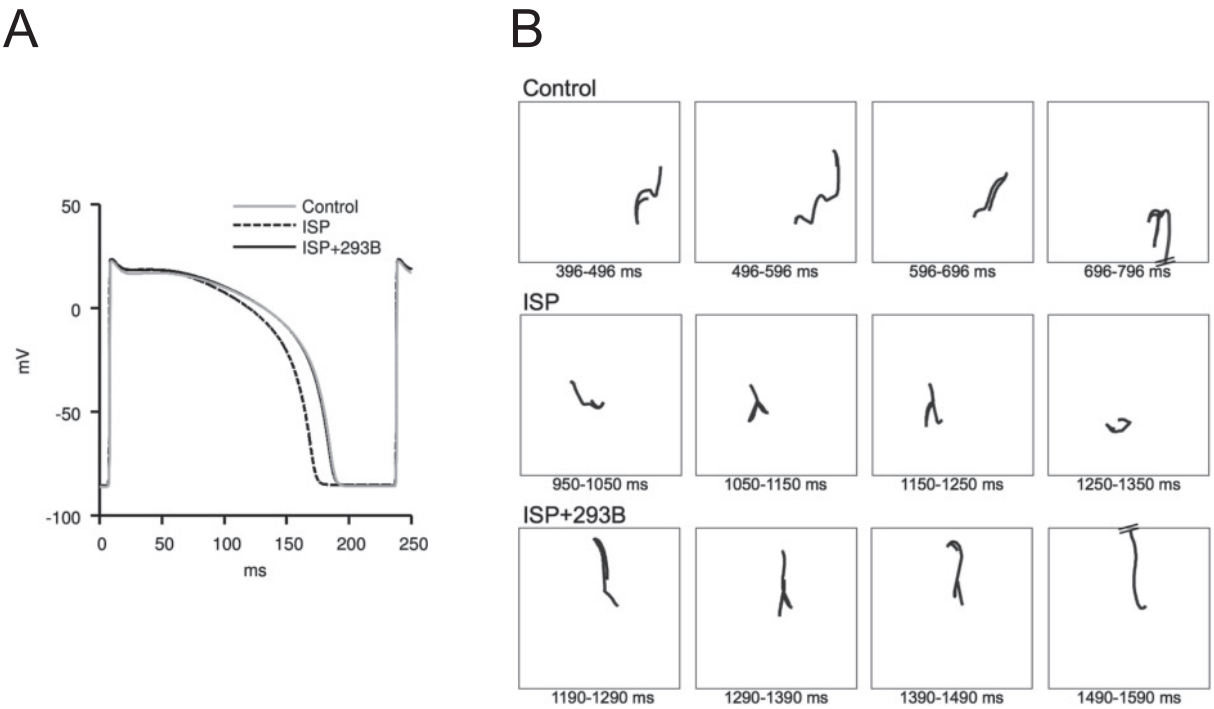

Fig. 6. Action potentials and SW dynamics in numerical simulation. A: Action potentials in a single cell model under constant stimulation (BCL, 230 ms). Action potentials before (control), after application of isoproterenol (ISP) alone, and after additional application of chromanol 293B (293B) are superimposed. ISP shortened APD_{90} by 9% from the control, and additional application of 293B reversed the APD change. B: Trajectories of the phase singularity (PS) point during SW reentry induced in a 2-dimensional tissue sheet model. A consecutive series of PS trajectories for a total of 400 ms (100 ms in each panel) are illustrated by solid lines before (control, top), after application of ISP alone (middle), and after additional application of 293B (bottom). =: rotor termination by PS collision with the tissue boundary. Numerals below each panel indicate time after application of cross-field stimulation. In the three conditions, cross-field stimulation induced a counterclockwise rotor around the center of the tissue. In the control, the rotor exhibited considerable meandering and self-terminated approximately 0.8 s after induction by collision with the lower tissue boundary. SW reentry induced in the presence of ISP alone was more stable (less meandering), and lasted longer than 2 s. SW reentry after additional application of 293B showed remarkable meandering again and self-terminated approximately 1.3 s after induction by collision with the upper tissue boundary.

ration in cardiac cells by this compound is much less than that by 2,3-butanedione monoxime (BDM) (22). The VTs induced under control conditions were unstable and terminated soon (VTs lasting > 5 s were only 3%). These characteristics deviate from those observed in our previous studies in a similar rabbit 2-dimensional ventricular myocardium in the presence of BDM, where VTs were more stable and lasted longer (VTs lasting > 30 s were 17% – 29%) (18, 19). The slope of APD restitution of ventricular muscle, which is known to determine the stability of wavefronts during functional reentry (33), was shown to be reduced significantly by BDM in favor of its stabilization, whereas unaffected or increased by cytochalasin D (22, 34).

VTs induced after single treatment with ISP were more stable and lasted longer than without ISP. SWs during the VTs were characterized by shorter FBL, a shorter VTCL, and less PS meandering. These changes are attributable mainly to ISP-induced shortening of APD. The FBL near the rotation center of SWs is kept refractory by preceding excitations (19), and APD abbreviation will shorten this FBL, giving rise to a shortening of path length of reentry.

Additional application of 293B to ISP-treated hearts reversed the ISP actions; SWs became unstable again as they were prior to ISP application, showing considerable drift and terminated soon after collision with anatomical boundaries. This reversal is most likely explained by the drug-induced prolongation of APD, which will prolong wavelength. It has been demonstrated in our previous studies in a similar 2-dimensional subepicardial layer of rabbit ventricular myocardium that APD (and wavelength) prolongation by either I_{Kr} blockade or moderate hypothermia destabilizes SWs and facilitates their meandering, leading to their spontaneous termination by collision with anatomical boundaries (7, 18). In contrast, a

shortening of APD by an L-type Ca^{2+}-channel blocker (verapamil) was shown to stabilize SWs and to increase the sustainability of VTs (19). It has also been demonstrated in theoretical studies on a 2-dimensional myocardial tissue model of finite size that APD prolongation by blockade of potassium currents destabilizes SW reentry and facilitates its early termination, indicating that maintenance of the reentrant arrhythmia critically depends on the ratio between tissue mass and wavelength (35). Our 2-dimensional mathematical model analysis is in line with this interpretation, since APD shortening by ISP and its reversal by 293B were associated with stabilization/destabilization of rotors in favor of their persistence and termination, respectively.

APD gradient near the SW rotation center

We demonstrated previously that nifekalant, a specific I_{Kr}-blocker, caused destabilization and early termination of SW reentry (7). This action was, however, associated with frequent break-up of wave fronts in the arm of SWs, giving rise to an increase in the wave breaks (7). In contrast, application of 293B in the presence of ISP caused destabilization and early termination of SW reentry without increasing such wave breaks. This may be explained by different contributions of I_{Kr} and I_{Ks} to the repolarization of action potential in the center and periphery of the SW reentrant circuits. Previous computer simulation studies using mathematical models in 2-dimensional cardiac tissue have shown that action potentials near the rotation center of SW reentry have less negative diastolic potential associated with moderate prolongation of APD, as a result of electrotonic depolarizing influence from surrounding tissue (29, 36). Electrotonic depolarization in the rotation center was also suggested in microelectrode experiments (37). On the other hand, I_{Ks} accumulation under high frequency excitation (12, 15) is considered to be increased in the region of less negative diastolic potential (13) and may counteract the electrotonic APD prolongation. In the presence of ISP, where I_{Ks} is largely enhanced and its deactivation is slowed down in favor of its accumulation (13), the latter effect may overcome the former one, giving rise to shorter APD in the center than periphery. Consequently, front-tail interactions near the rotation center would be reduced in favor of SW stabilization. Reversal of ISP action on the spatial gradient of APD after additional application of 293B is consistent with this interpretation. In our 2-dimensional model analysis, APD abbreviation by ISP was, in concordance with our experimental observations, more pronounced near the SW rotation center, and the change was reversed by 293B, suggesting a greater contribution of I_{Ks} on repolarization in the center than periphery.

Clinical implication

The present study suggest that β-adrenergic stimulation stabilizes SW reentry most likely though an enhancement of I_{Ks} and that blockade of I_{Ks} may be a promising therapeutic modality to prevent perpetuation of ventricular tachyarrhythmias under high sympathetic activity. However, care should be taken in extrapolating our observations into clinical practice. In normal human ventricular myocardium, I_{Ks} acts to prevent excessive APD prolongation under a variety of conditions such as hypokaremia, after a long pause of heart rhythm, under drug treatment with Class III action, and inherited mutations of ion channel proteins (38). In congenital long QT syndrome patients with I_{Ks} deficiency (LQT1), the incidence of arrhythmia events and sudden death are reported to be associated with high sympathetic activity (e.g., physical or emotional stress) (39). In a canine LV wedge preparation model of LQT1, Shimizu et al. (40, 41) demonstrated that addition of ISP in the presence of 293B shortened APD in epicardial and endocardial muscle layers, whereas it prolonged APD in the midmyocardial layer, causing an increase of transmural dispersion of repolarization (TDR) in favor of occurrence of TdP. These observations seem to indicate that pharmacological blockade of I_{Ks} may have a proarrhythmic propensity, especially when ventricular repolarization reserve is compromised (38, 42, 43). In diseased hearts, however, the scenario is more complex. Pajouh et al. (44) demonstrated in LV wedge preparations from pacing-induced heart failure dogs, unlike in those from normal dogs, addition of ISP after pretreatment with 293B did not increase TDR. In exercising dogs with healed anterior-wall myocardial infarction and superimposed ischemia (transient occlusion of left circumflex coronary artery), Lynch et al. (45) demonstrated that L-768,673, a selective I_{Ks}-blocker, significantly reduced the occurrence of ischemic VF. In an in vivo rabbit model, HMR1556, another selective I_{Ks}-blocker was shown to reduce ventricular defibrillation threshold in association with a reversal of ISP-induced APD shortening (16). The antiarrhythmic/proarrhythmic properties of I_{Ks}-blockers under high sympathetic activity may be affected by different pathological conditions and warrant further evaluation.

Limitations

In this study using a 2-dimensional subepicardial layer of rabbit ventricular myocardium, 293B reversed the ISP action to stabilize SW reentry, suggesting potential efficacy of I_{Ks} blockade in the treatment of VT/VF. Extending these results to 3-dimensional hearts, especially in larger animals including humans, is not straightforward. When there is sufficient tissue mass, the chance of spontaneous termination of rotors through collision with ana-

tomical boundaries would be reduced, whereas the enhancement of rotor drift and SW instability might promote transition from VT to VF. We used ISP to mimic high sympathetic tone, but their effects on the heart are different in terms of spatial heterogeneity. We used cytochalasin D as an excitation–contraction uncoupler, which is known to alter Ca^{2+} dynamics of cardiomyocytes (46). Accordingly, proarrhythmic action by ISP through modulation of intracellular Ca^{2+} dynamics might have been modified. Despite these limitations, the present study provides a new perspective on the pharmacological regulation of reentrant arrhythmias under high sympathetic activity.

Acknowledgments

This study was financially supported by Grants-in-Aid for Scientific Research (B) 19390210 and (C) 20590860 from the Japanese Society for Promotion of Sciences and Grant-in-Aid for Scientific Research on Innovative Area 2213610 from the Ministry of Education, Culture, Sports, Science, and Technology, Japan.

References

1 Schwartz PJ, Zipes DP. Autonomic modulation of cardiac arrhythmias. In: Zipes DP, Jalife J, editors. Cardiac electrophysiology: from cell to bedside. 3rd ed. Philadelphia: WB Saunders; 2000. p. 300–314.

2 Poole JE, Bardy GH. Sudden cardiac death. In: Zipes DP, Jalife J, editors. Cardiac electrophysiology: from cell to bedside. 3rd ed. Philadelphia: WB Saunders; 2000. p. 615–640.

3 Jalife J. Ventricular fibrillation: mechanisms of initiation and maintenance. Ann Rev Physiol. 2000;62:25–50.

4 Weiss JN, Qu Z, Chen PS, Lin SF, Karagueuzian HS, Hayashi H, et al. The dynamics of cardiac fibrillation. Circulation. 2005; 112:1232–1240.

5 Nerbonne JM, Kass RS. Molecular physiology of cardiac repolarization. Physiol Rev. 2005;85:1205–1253.

6 Dorian P, Newman D. Rate dependence of the effect of antiarrhythmic drugs delaying cardiac repolarization: an overview. Europace. 2000;2:277–285.

7 Yamazaki M, Honjo H, Nakagawa H, Ishiguro YS, Okuno Y, Amino M, et al. Mechanisms of destabilization and early termination of spiral wave reentry in the ventricle by a class III antiarrhythmic agent, nifekalant. Am J Physiol Heart Circ Physiol. 2007;292:H539–H548.

8 Roden DM. Drug-induced prolongation of the QT interval. N Engl J Med. 2004;350:1013–1032.

9 Sanguinetti MC, Jurkiewicz NK, Scott A, Siegl PK. Isoproterenol antagonizes prolongation of refractory period by the class III antiarrhythmic agent E4031 in guinea pig myocytes. Mechanism of action. Circ Res. 1991;68:77–84.

10 Li RA, Chiamvimonvat N. Adrenergic signaling and cardiac ion channels. In: Zipes DP, Jalife J, editors. Cardiac electrophysiology: from cell to bedside. 5th ed. Philadelphia: WB Saunders; 2009. p. 373–380.

11 Mantravadi R, Gabris B, Liu T, Choi B-R, de Groat WC, Ng GA, et al. Autonomic nerve stimulation reverses ventricular repolarization sequence in rabbit hearts. Circ Res. 2007;100:e72–e80.

12 Jurkiewicz NK, Sanguinetti MC. Rate-dependent prolongation of cardiac action potentials by a methanesulfonanilide class III antiarrhythmic agent. Specific block of rapidly activating delayed rectifier K^+ current by dofetilide. Circ Res. 1993;72:75–83.

13 Stengl M, Volders PG, Thomsen MB, Spätjens RL, Sipido KR, Vos MA. Accumulation of slowly activating delayed rectifier potassium current (I_{Ks}) in canine ventricular myocytes. J Physiol. 2003;551:777–786.

14 Bosch RF, Gaspo R, Busch AE, Lang HJ, Li GR, Nattel S. Effects of the chromanol 293B, a selective blocker of the slow, component of the delayed rectifier K^+ current, on repolarization in human and guinea pig ventricular myocytes. Cardiovasc Res. 1998;38:441–450.

15 Lu Z, Kamiya K, Opthof T, Yasui K, Kodama I. Density and kinetics of I_{Kr} and I_{Ks} in guinea pig and rabbit ventricular myocytes explain different efficacy of I_{Ks} blockade at high heart rate in guinea pig and rabbit: implications for arrhythmogenesis in humans. Circulation. 2001;104:951–956.

16 So PP, Backx PH, Hu XD, Dorian P. I_{Ks} block by HMR 1556 lowers ventricular defibrillation threshold and reverses the repolarization shortening by isoproterenol without rate-dependence in rabbits. J Cardiovasc Electrophysiol. 2007;18:750–756.

17 Sun ZQ, Thomas GP, Antzelevitch C. Chromanol 293B inhibits slowly activating delayed rectifier and transient outward currents in canine left ventricular myocytes. J Cardiovasc Electrophysiol. 2001;12:472–478.

18 Harada M, Honjo H, Yamazaki M, Nakagawa H, Ishiguro YS, Okuno Y, et al. Moderate hypothermia increases the chance of spiral wave collision in favor of self-termination of ventricular tachycardia/fibrillation. Am J Physiol Heart Circ Physiol. 2008; 294:H1896–H1905.

19 Ishiguro YS, Honjo H, Opthof T, Okuno Y, Nakagawa H, Yamazaki M, et al. Early termination of spiral wave reentry by combined blockade of Na^+ and L-type Ca^{2+} currents in a perfused two-dimensional epicardial layer of rabbit ventricular myocardium. Heart Rhythm. 2009;6:684–692.

20 Takanari H, Honjo H, Takemoto Y, Suzuki T, Kato S, Harada M, et al. Bepridil facilitates early termination of spiral-wave reentry in two-dimensional cardiac muscle through an increase of intercellular electrical coupling. J Pharmacol Sci. 2011;115:15–26.

21 Yamazaki M, Honjo H, Ashihara T, Harada M, Sakuma I, Nakazawa K, et al. Regional cooling facilitates termination of spiral-wave reentry through unpinning of rotors in rabbit hearts. Heart Rhythm. 2012;9:107–114.

22 Lee MH, Lin SF, Ohara T, Omichi C, Okuyama Y, Chudin E, et al. Effects of diacetyl monoxime and cytochalasin D on ventricular fibrillation in swine right ventricles. Am J Physiol Heart Circ Physiol. 2001;280:H2689–H2696.

23 Gray RA, Pertsov AM, Jalife J. Spatial and temporal organization during cardiac fibrillation. Nature. 1998;392:75–78.

24 Shannon TR, Wang F, Puglisi J, Weber C, Bers DM. A mathematical treatment of integrated Ca dynamics within the ventricular myocyte. Biophys J. 2004;87:3351–3371.

25 Trautwein W, Hescheler J. Regulation of cardiac L-type calcium current by phosphorylation and G proteins. Annu Rev Physiol. 1990;52:257–274.

26 Yazawa K, Kameyama M. Mechanism of receptor-mediated modulation of the delayed outward potassium current in guinea-pig ventricular myocytes. J Physiol. 1990;421:135–150.

27 Thomas D, Zhang W, Karle CA, Kathöfer S, Schöls W, Kübler W, et al. Deletion of protein kinase A phosphorylation sites in the HERG potassium channel inhibits activation shift by protein kinase A. J Biol Chem. 1999;274:27457–27462.
28 Thomas D, Kiehn J, Katus HA, Karle CA. Adrenergic regulation of the rapid component of the cardiac delayed rectifier potassium current, I_{Kr}, and the underlying hERG ion channel. Basic Res Cardiol. 2004;99:279–287.
29 Qu Z, Xie F, Garfinkel A, Weiss JN. Origins of spiral wave meander and breakup in a two-dimensional cardiac tissue model. Ann Biomed Eng. 2000;28:755–771.
30 Beaumont J, Jalife J. Rotors and spiral waves in two dimensions. In: Zipes DP, Jalife J, editors. Cardiac electrophysiology: from cell to bedside. 3rd ed. Philadelphia: WB Saunders; 2000. p. 327–335.
31 Hume JR, Harvey RD. Chloride conductance pathways in heart. Am J Physiol Cell Physiol. 1991;261:C399–C413.
32 Takano M, Noma A. Distribution of the isoprenaline-induced chloride current in rabbit heart. Pflugers Arch. 1992;420: 223–226.
33 Weiss JN, Garfinkel A, Karagueuzian HS, Qu Z, Chen PS. Chaos and the transition to ventricular fibrillation: a new approach to antiarrhythmic drug evaluation. Circulation. 1999;99:2819–2826.
34 Riccio ML, Koller ML, Gilmour RF Jr. Electrical restitution and spatiotemporal organization during ventricular fibrillation. Circ Res. 1999;84:955–963.
35 Qu Z. Critical mass hypothesis revisited: role of dynamical wave stability in spontaneous termination of cardiac fibrillation. Am J Physiol Heart Circ Physiol. 2006;290:H255–H263.
36 Grzeda KR, Anumonwo JM, O'Connell R, Jalife J. A single-cell model of phase-driven control of ventricular fibrillation frequency. Biophys J. 2009;96:2961–2976.
37 Schalij MJ, Boersma L, Huijberts M, Allessie MA. Anisotropic reentry in a perfused 2-dimensional layer of rabbit ventricular myocardium. Circulation. 2000;102:2650–2658.
38 Jost N, Papp JG, Varró A. Slow delayed rectifier potassium current (I_{Ks}) and the repolarization reserve. Ann Noninvasive Electrocardiol. 2007;12:64–78.
39 Antzelevitch C. Mechanisms of cardiac arrhythmias and conduction disturbances. In: Fuster V, O'Rourke RA, Walsh RA, Poole-Wilson P, editors. Hurst's the heart. 12th ed. New York: McGraw-Hill; 2008. p. 913–945.
40 Shimizu W, Antzelevitch C. Cellular basis for the ECG features of the LQT1 form of the long-QT syndrome: effects of β-adrenergic agonists and antagonists and sodium channel blockers on transmural dispersion of repolarization and torsade de pointes. Circulation. 1998;98:2314–2322.
41 Shimizu W, Antzelevitch C. Differential effects of beta-adrenergic agonists and antagonists in LQT1, LQT2 and LQT3 models of the long QT syndrome. J Am Coll Cardiol. 2000;35:778–786.
42 Volders PG, Stengl M, van Opstal JM, Gerlach U, Spätjens RL, Beekman JD, et al. Probing the contribution of I_{Ks} to canine ventricular repolarization: key role for beta-adrenergic receptor stimulation. Circulation. 2003;107:2753–2760.
43 Jost N, Virág L, Bitay M, Takács J, Lengyel C, Biliczki P, et al. Restricting excessive cardiac action potential and QT prolongation: a vital role for I_{Ks} in human ventricular muscle. Circulation. 2005;112:1392–1399.
44 Pajouh M, Wilson LD, Poelzing S, Johnson NJ, Rosenbaum DS. I_{Ks} blockade reduces dispersion repolarization in heart failure. Heart Rhythm. 2005;2:731–738.
45 Lynch JJ Jr, Houle MS, Stump GL, Wallace AA, Gilberto DB, Jahansouz H, et al. Antiarrhythmic efficacy of selective blockade of the cardiac slowly activating delayed rectifier current, I_{Ks}, in canine models of malignant ischemic ventricular arrhythmia. Circulation. 1999;100:1917–1922.
46 Rueckschloss U, Isenberg G. Cytochalasin D reduces Ca^{2+} currents via cofilin-activated depolymerization of F-actin in guinea-pig cardiomyocytes. J Physiol. 2001;537:363–370.